A Nonlinear Dissipation Function due to Wave Breaking

Mark A. Donelan
Rosenstiel School for Marine and Atmospheric Science
University of Miami

1. Introduction

The "radiative transfer equation" is the physical basis for most modern numerical wave forecasting:

$$\left\{\frac{\partial}{\partial t}+\left(C_g+U\right)\bullet\frac{\partial}{\partial x_i}-\left(\nabla_x\Omega\right)\bullet\frac{\partial}{\partial k}\right\}F(k)=S_{in}+S_{nl}+S_{wb}+S_{bf} \qquad (1)$$

The left hand side describes the conservation of wave energy as the wave field evolves in space and time, while the right hand side consists of sources and sinks. The term S_{wb} is the loss of energy through dissipation due to wave breaking and is the subject of this paper. The other source/sink terms – input from the wind, nonlinear wave-wave interactions and bottom friction – are all active areas of research, but there is little doubt that the least well understood term is the "wave breaking dissipation" term [Komen et al., 1994]. This is due largely to the extreme difficulty of measuring the dissipation of waves in the field. In the laboratory some idealized experiments have been performed wherein prescribed packets of waves are made to coalesce and break and measurements of the wave energy spectra are made upstream and downstream of the breaking region (Rapp and Melville, 1990; Pierson et al., 1992). The differences between the upstream and downstream measurements are taken to be representative of the rate of energy dissipation through wave breaking, on the grounds that wave dissipation in the breaking region is a much faster process than any other source/sink term. Of course, these packets do not simulate the complex processes of wave dissipation in a wind-forced wave field, and therefore can act only as guidance in understanding S_{wb}. How can one obtain observational evidence for the form of S_{wb}?

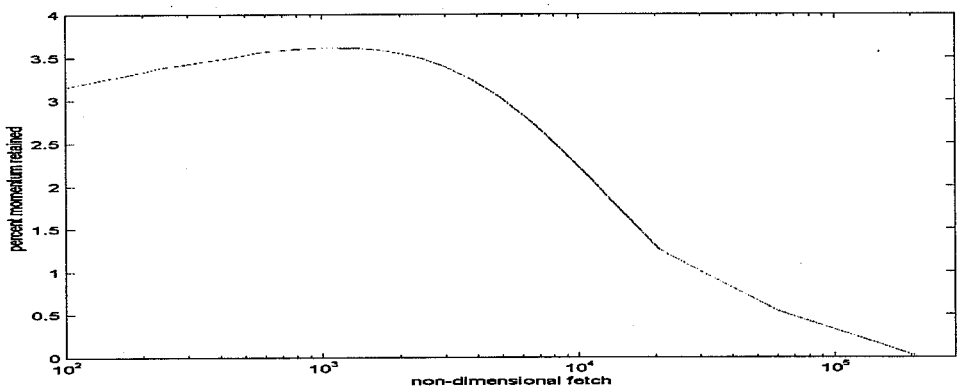

Figure 1. The percentage of momentum from the wind that is retained by the wave field at various stages of development from very short fetch on the left to full development on the right where, by definition no further increase in wave momentum is realized with increasing fetch.

As it happens, nature has conspired to help us resolve this question. It is well known that, although wind-driven waves can grow to ship-destroying monsters, their growth is slow compared to the overall momentum transfer between wind and waves, being at most a few percent of the latter (Hasselmann et al., 1973, Donelan, 1998) Figure 1 (adapted from Donelan, 1998) illustrates the fraction of momentum from the wind that is retained by the wave field in steady-state, fetch-limited conditions. The point of full development is also shown where, by definition, there is no further change in the wave field so that the momentum retained is zero. In strong wind conditions the momentum from the wind is delivered initially to waves (via form drag) and most of this (1 minus that retained) is delivered locally to the water column via the process of wave breaking or S_{wb}. In other words, the source/sink function processes on the right hand side of (1) tend to cancel each other in steady-state, fetch-limited, deep water or uniform depth conditions, without currents, U.

$$C_g \bullet \frac{\partial F(k)}{\partial x_i} = S_{in} + S_{nl} + S_{wb} + S_{bf} \leq 0.05 S_{in} \tag{2}$$

Calculations of bottom friction, S_{bf} (Komen et al., 1994) indicate that it is very weak compared to S_{in} when waves are steep enough or forced strongly enough to produce white-capping. The nonlinear wave-wave interactions have no net effect on the overall energy, but they can transfer energy within the spectrum. Thus in strong winds and steady-state, fetch-limited, deep water or uniform depth conditions, with no currents the balance is between these terms:

$$C_g \bullet \frac{\partial F(k)}{\partial x_i} = S_{in} + S_{nl} + S_{wb} \leq 0.05 S_{in} \tag{3}$$

Observational evidence for S_{in} has accumulated over the past decades and, coupled with the results of numerical modeling, the form and strength of S_{in} can be said to be quite well known. Based on laboratory experiments, Donelan (1999) gives:

$$S_{in} = 0.28 \frac{\rho_a}{\rho_w} \left| \frac{U(\lambda/2)}{c} - 1 \right| \left(\frac{U(\lambda/2)}{c} - 1 \right) \omega F(k) \tag{4}$$

where c is the phase propagation speed, ω the intrinsic frequency of waves of wavenumber k, and $U(\lambda/2)$ the wind speed at ½ wavelength height.

The advective term (left hand side of equation (3), F_{adv} for short) is small compared to S_{in} but, nevertheless, may be computed quite accurately from "fetch laws". One such fetch law (Donelan et al., 1992) is given as a continuous function from very fetch-limited to fully developed and may be applied to compute the advective term.

Thus, in regions of the spectrum where S_{nl} is relatively small S_{wb} may be determined by equating it to F_{adv} - S_{in} via equation (3). One such place is at the spectral peak, where calculations indicate the value of S_{nl} goes through zero for young waves. The relative magnitude of these terms is illustrated in Figure 2, in which the wind speed at 10 meters is held constant at 10m/s as the waves develop. Each term is normalized by the kinematic stress, u_*^2 so that, for example, the magenta curve, S_{in} represents the contributions to the stress versus frequency. The spectrum of surface elevation is not shown, but the location of its peak is indicated by the vertical dotted line. To the left of the peak on the forward face the wave steepness is very low and thus S_{wb} is expected to be negligible. Therefore an estimate of the positive lobe of S_{nl} may be obtained from F_{adv} - S_{in} in this region of the spectrum. This is shown by the cyan curve, which is plotted with its sign reversed for

clarity. Theoretical calculations of the weak nonlinear wave-wave interactions are interesting and have stimulated a great deal of progress in the methodology of numerical wave prediction. However, the theory is based on assumptions that are not in general met in an actively growing wave field – assumptions of homogeneity and random phases among components as well as the direct application of the linear dispersion relation in spite of the strongly varying vertical acceleration experienced by short waves riding on longer components. Consequently, it behooves us to test its predictions against observations. This is not the place for an exhaustive study of that type, but it is clear from Figure 2 that the positive low frequency lobe of S_{nl} is small compared to the broad peak of S_{in} and since S_{nl} reaches its largest values near the spectral peak, it will be dwarfed by S_{in} elsewhere in the spectrum. I have assumed that the theoretical calculations of S_{nl} yield the correct shape, but not the amplitude. This should be subjected to rigorous experimental tests. The wave community seems oddly attached to theoretical calculations of S_{nl} that have not been verified experimentally. Instead, a truly amazing effort has been expended on improved approximations of the "exact" theoretical result, when the latter has not had the benefit of experimental verification. It should be noted that there are other wave-wave interactions not included in the theory behind S_{nl} such as the strong interactions associated with wave breaking that move energy away from the peak to lower and higher frequencies (Pierson et al., 1992). Thus the estimates of S_{nl} (the weak quartic wave-wave interaction) given in Figure 2 are overestimates. With this in mind, a balance between S_{in} - F_{adv} and S_{wb} seems justified at the peak for young waves. Well above the peak for all stages of development, both F_{adv} and S_{nl} are small compared to S_{in} allowing a direct balance between S_{in} and S_{wb}.

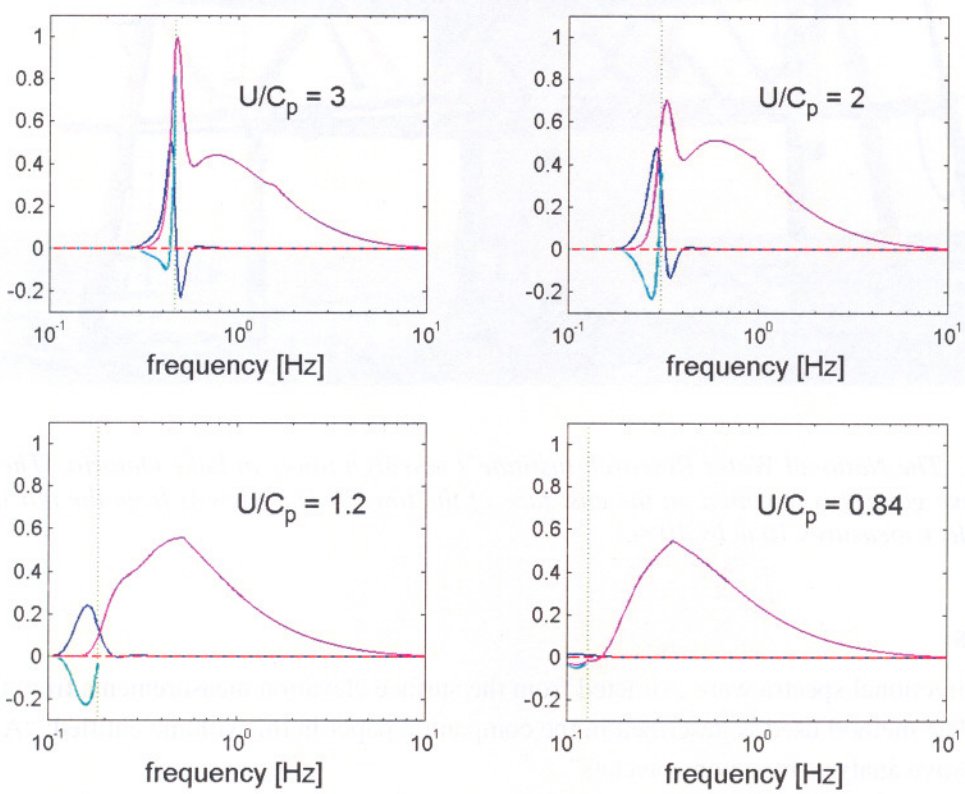

Figure 2. The spectral distribution of momentum input to waves from wind S_{in} (magenta); of the momentum retained by waves as they develop along fetch (blue). The four panels are for different stages of wave development as indicated and the vertical dashed line indicates the location of the spectral peak. Shown only to the left of the spectral peak is the difference of the wind input and the momentum retained (cyan).

2. Measurements

The data used here for illustration were obtained from the research tower in Lake Ontario during the Water-Air Vertical Exchange Studies (WAVES) experiment n 1987 – the third and final year (see Figure 3). The to wer is fixed to the bottom in 12 m of water at the western end of Lake Ontario, 1.1 km from the shore. It is exposed to fetches that vary from 1.1 km for westerly winds to 300 km for ENE winds. Wave directional measurements were made with an array of six capacitance wave gauges arranged in a centered pentagon of radius 25 cm. The wind speed and wind stress were measured by means of the bivane anemometer on the top of the mast at 11 meters above the mean water level.

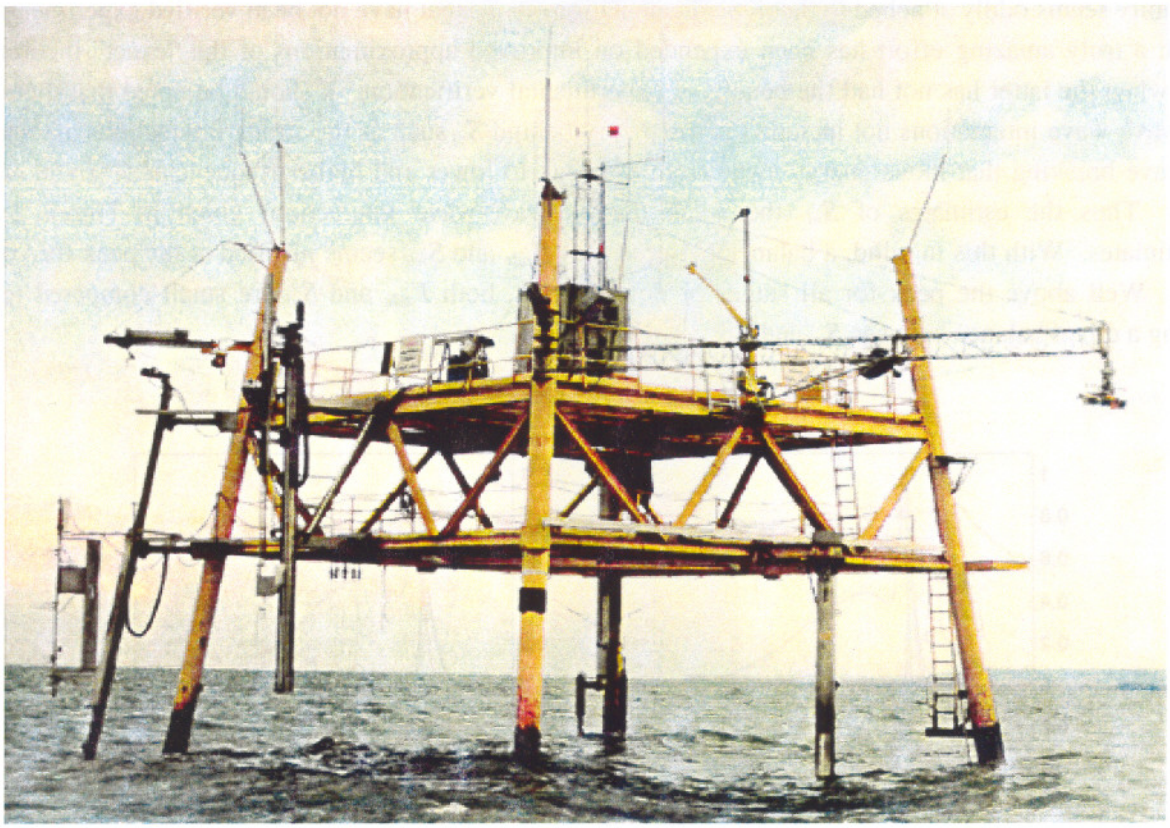

Figure 3. The National Water Research Institute's research tower in Lake Ontario. The array of six wave gauges is mounted on the east face of the tower. This view is from the north-west. The top deck measures 10 m by 10 m.

3. Results

Wavenumber directional spectra were extracted from the surface elevation measurements from the array of 6 wave gauges. The method used is described in the companion paper in this volume entitled: "A new method for directional wave analysis based on wavelets".

There were 112 hour-long runs in this data set. In order to examine the wave-breaking dissipation at the peak in the manner described above, the following requirements were placed on the runs in the set: (a) wind speed greater than 6 m/s; (b) wind direction and peak wave direction are within 30 degrees of each other; (c) wind speed at least 10% greater than the wave speed at the spectral peak. Twenty-seven runs met these requirements and they were used to compare S_{in} and S_{wb}. In this paper all references to the wavenumber

spectra $F(k)$ refer to the spectral value averaged over $\pm$ 20 degrees about the peak direction at that wavenumber. Its units are m^4.

The form of S_{in} is given in equation (4). S_{wb} is assumed to have the following form, being dependent on the degree of saturation or the curvature spectrum, $B(k) = k^4 F(k)$:

$$S_{wb}(k) = -A\omega(k)F(k)[B(k)]^n \tag{5}$$

where the constant A and the power n are to be determined empirically below. Figure 4 shows the comparison of S_{in} and S_{wb} for dissipation being linear in the spectral density (n = 0) and dissipation being dependent on the degree of saturation (n = 2.5). The latter choice yielded the best agreement between S_{in} and S_{wb} as shown in panel (a). The values of A in these cases was determined to be 0.00036 and 36 respectively.

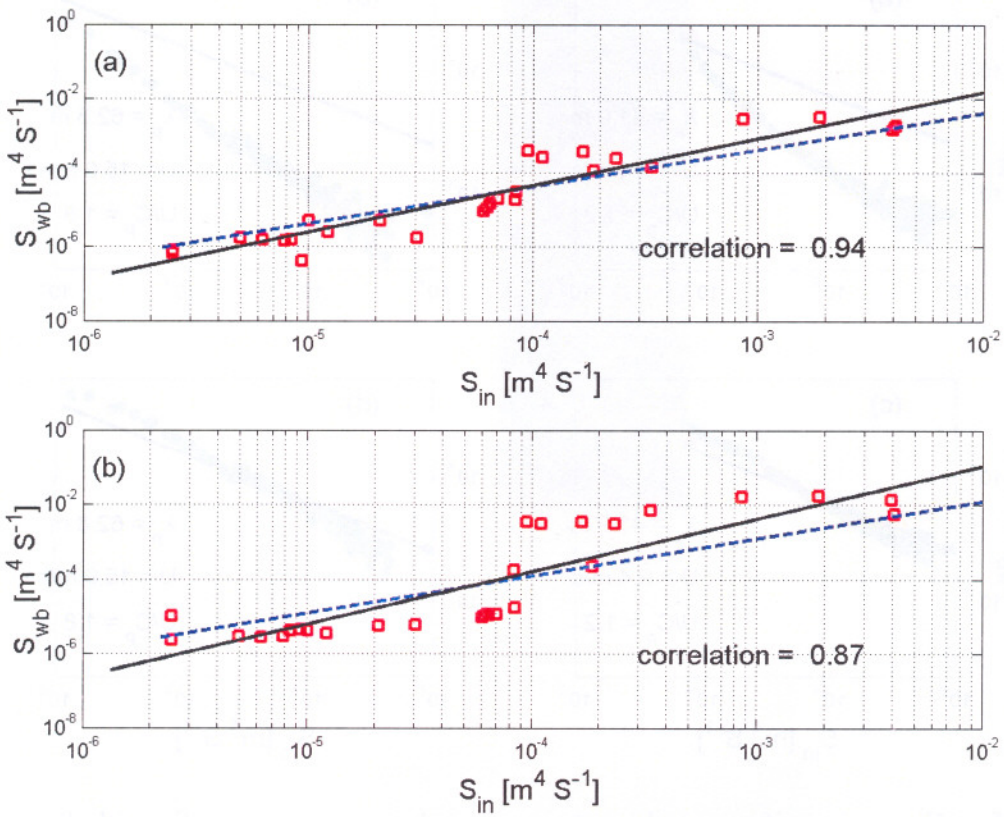

Figure 4. Comparison of the wind input term at the peak of the spectrum S_{in} *with dissipation at the peak of the spectrum* S_{wb} *calculated from equation (5). In panel (a) the power,* n *of the degree of saturation is 2.5, while in panel (b),* n *is zero corresponding to a dissipation rate that is linear in the spectrum. The black line is the linear regression line of the logarithms of* S_{in} *and* S_{wb} *; while the blue line is the line of perfect agreement.*

Above the peak the comparison between input (equation (4)) and dissipation calculated using equation (5) (with n = 2.5 and A = 36) suggests that the dissipation rate does not keep up with the wind input. The reason for this is that the dissipation rate for these short quasi-saturated waves is modulated by the straining action of the longer waves. On the forward face of the longer waves the short waves slopes are increased and, being on average steep enough to break intermittently, their breaking intensity is increased. Conversely, on the rear faces of the longer waves the short wave slopes are reduced and they are able to grow further in

response to the wind. This latter process is relatively slow compared to the energy loss in breaking, so that short waves modulated in this way suffer a net reduction in energy density. Consequently equation (5) needs to be modified to account for this long/short wave interaction. I assume that the mean square slope, in the direction of propagation of a particular short wave, of all longer waves (***mss(k)***) modifies the dissipation rate in the following way:

$$S_{wb}(k)=-36\omega(k)F(k)[\{1+500mss(k)\}^2 B(k)]^{2.5} \tag{6}$$

where the constant 500 and the exponent 2 were determined by fitting to the observed spectra and calculated wind inputs. Equation (6) expresses the idea that the longer waves bring the shorter waves closer to saturation.

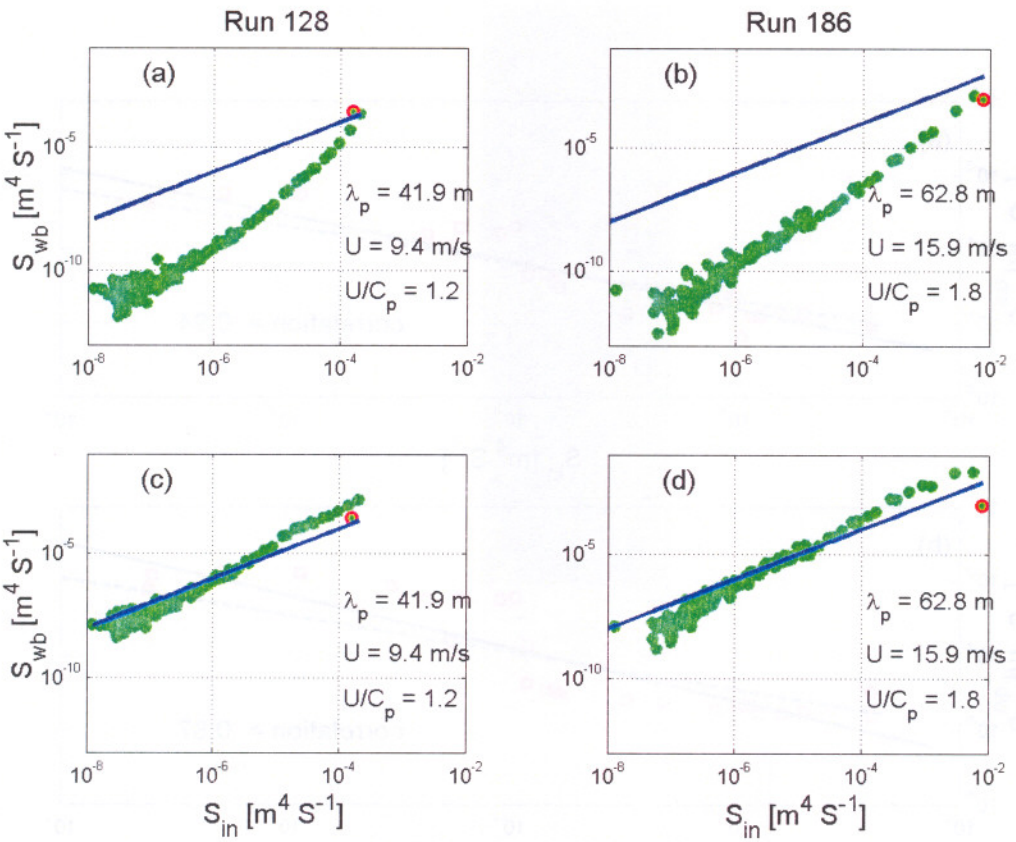

Figure 5a. Comparison of the wind input term over the entire spectrum S_{in} *with dissipation over the entire spectrum* S_{wb} *calculated from equation (6). The runs shown have long waves at the peak with 2 quite different forcing rates as shown. In panels (a) and (b) no adjustment for the slope of the longer waves has been made; while in panels (c) and (d) the effect of slope given in equation (6) is included. The point corresponding to the peak is shown as a red circle. The blue line is the line of perfect agreement.*

Figures 5a and 5b illustrate the improvement in the fit of input and dissipation over the whole spectrum for both long and short waves at various stages of development.

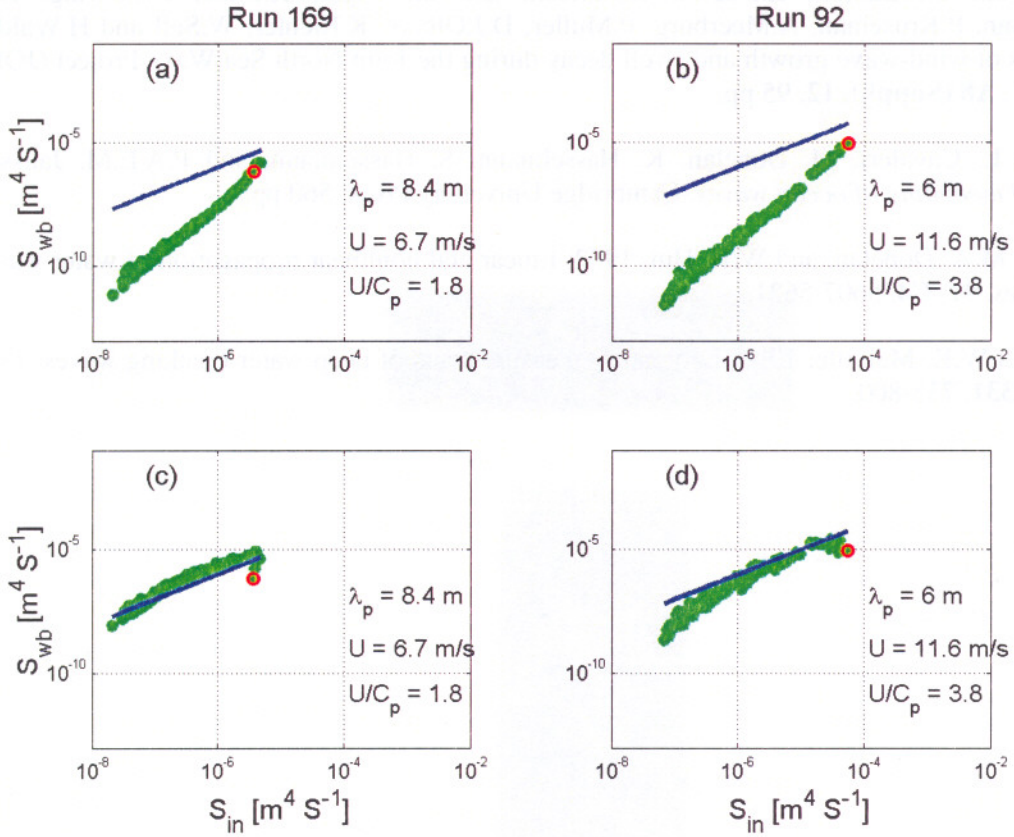

Figure 5b. Comparison of the wind input term over the entire spectrum S_{in} *with dissipation over the entire spectrum* S_{wb} *calculated from equation (6). The runs shown have short waves at the peak with 2 quite different forcing rates as shown. In panels (a) and (b) no adjustment for the slope of the longer waves has been made; while in panels (c) and (d) the effect of slope given in equation (6) is included. The point corresponding to the peak is shown as a red circle. The blue line is the line of perfect agreement.*

4. Summary

The illusive "dissipation due to wave breaking" source term in the energy balance equation for wind generated water waves has been explored from field data. By invoking a balance between wind input and dissipation in certain regions of the spectrum, the form and magnitude of the dissipation term has been determined and given in equation (6). Further analysis is planned to determine the various empirical constants with greater statistical reliability.

Acknowledgments

I acknowledge the support from the U.S. Office of Naval Research through grant number N00014-97-1-0348.

References

Donelan, M.A., 1998: Air-water exchange processes. In: Physical Processes in Oceans and Lakes (J. Imberger, Ed.), *AGU Coastal and Estuarine Studies* **54**, 19-36.

Donelan, M.A., 1999: Wind-induced growth and attenuation of laboratory waves. In: *Wind-over-wave couplings: perspectives and prospects*. (S.G. Sajjadi, N.H.Thomas and J.C.R. Hunt, Eds), Clarendon Press, 183-194.

Donelan, M., M. Skafel, H. Graber, P. Liu, D. Schwab, and S. Venkatesh, 1992: On the Growth Rate of Wind-Generated Waves. *Atmos.-Ocean*, **30**, 457-478.

Hasselmann, K., T.P.Barnett, E.Bouws, H.Carlson, D.E.Cartwright, K.Enke, J.A.Ewing, H.Gienapp, D.E.Hasselmann, P.Kruseman, A.Meerburg, P.Muller, D.J.Olbers, K.Richter, W.Sell and H.Walden, 1973: Measurements of wind-wave growth and swell decay during the Joint North Sea Wave Project (JONSWAP). *Dt.Hydrogr.Z.*, **A8 (Suppl.), 12**, 95 pp.

Komen, G.J., L. Cavaleri, M. Donelan, K. Hasselmann, S. Hasselmann, and P.A.E.M. Janssen, 1994. *Dynamics and modelling of ocean waves*. Cambridge University Press, 560 pp.

Pierson, W.J., M.A. Donelan. and W.H. Hui, 1992: Linear and nonlinear propagation of water wave groups. *J. Geophys. Res.* **97, C4**, 5607-5621.

Rapp, R.J., and W.K. Melville, 1990: Laboratory measurements of deep-water breaking waves. *Phil. Trans. R. Soc. Lond.* **331**, 735-800.